

Largest Lyapunov exponent in molecular systems: Linear molecules and application to nitrogen clusters

F. Calvo*

Laboratoire Collisions, Agrégats, Réactivité, CNRS UMR 5589, Institut de Recherche sur les Systèmes Atomiques et Moléculaires Complexes, Université Paul Sabatier, 118 Route de Narbonne, F31062 Toulouse Cédex, France

(Received 19 March 1998)

The computation of the largest Lyapunov λ exponent is carried out for a Hamiltonian system made of linear molecules. The internal rotational degrees of freedom are described with unit vectors parallel to molecular axes. As an application, we investigate with classical molecular dynamics the behavior of λ with internal energy in small nitrogen clusters with 3 and 13 molecules. λ sharply rises when the molecular rotational degrees of freedom are released. However, no particular changes are observed at the solidlike-rigidlike phase transition. Thus the amount of chaos in the cluster seems mainly governed by the orientational degrees of freedom. [S1063-651X(98)01411-1]

PACS number(s): 05.45.+b, 05.70.Fh, 36.40.-c

I. INTRODUCTION

As an intermediate stage between the microscopic and bulk levels, clusters offer very peculiar chemical and physical behaviors. In particular, the study of phases and phase changes in these systems has led in the past decade to a fairly good understanding of how melting occurs far below the thermodynamic limit. However, most of the earliest investigations were carried out on simple atomic models such as the Lennard-Jones (LJ) or Morse potentials. These potentials are ideal for carrying out numerical experiments, and the physics of bulk fluids has been testing many theories and models with them. More recently, interest was granted to many other kinds of cluster species, ranging from ionic [1–3], metallic [4], fullerenes [5,6], water [7,8], and many others. Up to now, mostly Fuchs and co-workers have paid attention to van der Waals molecular clusters from the thermodynamic point of view [9–14]. These systems may exhibit very particular phases. For instance, large $(\text{SF}_6)_N$ clusters ($N \sim 10^3$) show two distinct ordered crystal-like phases in different ranges of temperature [10], whereas smaller sizes ($N \sim 10$) show featureless caloric curves [9]. Besides this solid-solid phase transition, an embryonic solid-plastic transition was found in nitrogen clusters [12]. The loss of orientational order in $(\text{N}_2)_{13}$ (near 10 K) was not found in $(\text{CO}_2)_{13}$, even though both clusters have identical S_6 structure at $T=0$ [12,14].

Among the various tools and parameters proposed to investigate the dynamics and thermodynamics of clusters, the Lyapunov exponents and the related Kolmogorov entropy have been the subject of several reports [15–28]. Defined as the exponential rate of convergence or divergence of neighboring trajectories in the phase space, the Lyapunov exponents are a measure of the degree of chaos in a dynamical system. Since there is a large difference in rigidity and ordering between a solid and a liquid, one can expect these numbers to be used as a probe of the solid-fluid phase tran-

sition, at least in the macroscopic limit [28–30]. However, because of relaxation phenomena, the computation of Lyapunov exponents is particularly difficult near a phase change [29].

Whenever a cluster melts, it may undergo an intermediate state which is a finite-size analog to the relaxation phenomena in bulk systems, known as dynamical coexistence [31]. In a range of energies or temperatures, the cluster permanently fluctuates back and forth between its solidlike and liquidlike phases. Coexistence in clusters is not a spatial notion related to phase separation, but is characteristic of how melting occurs at finite size, the cluster being entirely solidlike or entirely liquidlike at a given time. Of course, as the size increases, the temperature range of coexistence gets narrower to become finally reduced to the melting temperature.

Therefore, calculating Lyapunov exponents in clusters is not much easier than in periodic systems. Studies on bulk matter have clearly demonstrated the different behaviors of Lyapunov exponents across a phase transition [28–30,32,33]. However, the finite size of clusters and the strong sensitivity of the phase change upon the characteristics of the potential-energy surfaces make it hard to find such general laws at the level of a few atoms or molecules. Rare-gas clusters display very different variations of both the largest Lyapunov exponent λ and the Kolmogorov entropy K at melting, depending on their size [16,19–21,23,26]. Ionic clusters may undergo several hierarchical levels of melting [2,3], and display original variations of λ with energy, which have not been fully explained yet [3]. Using numerical simulations on Lennard-Jones (LJ) and metallic systems and the semianalytical results of a recent theory [34], Mehra and Ramaswamy [28] have investigated the respective contributions of local and parametric instabilities, especially near melting. In small clusters containing only a few atoms, local instability induced by negative curvature on the potential-energy surface is mainly responsible for chaos and exponentiating trajectories [18,19]. In larger systems and in the bulk, parametric instability induced by the fluctuations of positive curvature seems to dominate over the former [28].

The method mostly used for calculating Lyapunov spectra in numerical experiments is the tangent space method inde-

*Electronic address: florent@yosemite.ups-tlse.fr

pendently developed by Shimada and Nagishima [35] and by Benettin *et al.* [36]. This method allows us to compute the m largest Lyapunov exponents $\{\lambda_i\}$ of a dynamical system with dimension $n \geq m$, given its partial differential equations. Other methods, focusing on the Kolmogorov entropy, have been proposed in the cluster community [16]. Up to now, the tangent space method has been applied either to dissipative systems such as the Lorenz model [37] or to atomic or nuclear systems [16,21–27,29,30,33] and XY -like models [32], among others. Most of the time, and due to the heavy numerical cost involved in the computation, only the largest exponent λ_1 was sought. This is generally sufficient to characterize chaoticity in a quantitative way.

The purpose of this paper is to extend the tangent space approach to molecular systems where not only translational degrees of freedom are present, but also rotational degrees of freedom for each molecule. Here we focus on linear molecules; three-dimensional entities will be the subject of a following paper, the technique and basic equations being rather different with respect to the linear case. The paper is organized as follows. In the next section, we develop the standard method to include molecular rotation in the computation of Lyapunov exponents. Then we illustrate it with the study of phase changes in nitrogen clusters $(N_2)_n$ with $n = 3$ and 13. The results are given and discussed in Sec. III. Finally, we conclude and summarize in Sec. IV.

II. METHODOLOGY

Before coming to molecular systems, we start this section by recalling the main results of the tangent space method used to calculate the Lyapunov exponents in a Hamiltonian system. We consider a system of n dimensionless particles, evolving through the classical Hamilton's equations of motion. In condensed form, these equations can be written in the following way:

$$\frac{d\psi}{dt} = F(\psi), \quad (1)$$

where ψ is a $6n$ -vector of the phase space and F is a nonlinear function depending on ψ at time t . Obviously, solving Eq. (1) also requires an initial condition $\psi(0)$ for ψ . By definition, the largest Lyapunov exponent λ is the exponential rate of divergence of two initially close trajectories:

$$\lambda = \lim_{t \rightarrow \infty} \lim_{\delta\psi(0) \rightarrow 0} \frac{1}{t} \ln \frac{\|\delta\psi(t)\|}{\|\delta\psi(0)\|}, \quad (2)$$

where $\|\psi\| = \sqrt{\langle \psi | \psi \rangle}$ is a metric on the phase space and $\langle | \rangle$ is the associated scalar product. Of course, rigorously, λ depends on the choice of the initial condition $\psi(0)$ of the reference trajectory, but this difficulty can be eliminated for ergodic Hamiltonian systems [38]. In the following, we will assume ergodicity of our systems.

To avoid numerical difficulties due to the exponential divergence, we differentiate Eq. (1) to readily obtain the time evolution of the vector $\delta\psi(t)$ itself:

$$\frac{d\delta\psi}{dt} = \frac{\partial F}{\partial \psi} \delta\psi. \quad (3)$$

In the ‘‘tangent space,’’ one just has to follow the time evolution of the $6n$ -vector $\delta\psi(t)$ and to renormalize it periodically. Starting with $m \leq 6n$ orthogonal vectors $\{\delta\psi_i(0)\}$, a Gram-Schmidt orthonormalization procedure can be used to further estimate the $m - 1$ remaining largest Lyapunov exponents $\{\lambda_i\}$ of the system. Obviously, the numerical effort is also proportionally larger. In the following, we will only focus on the maximal exponent $\lambda = \lambda_1$.

For a Hamiltonian system interacting through the classical potential energy function V depending on the coordinates $\{\mathbf{r}_i\}$, $1 \leq i \leq n$, and with $\{\mathbf{p}_i\}$ the n linear momenta and $\{m_i\}$ the masses, we have $\psi = \{\mathbf{r}_i, \mathbf{p}_i\}$ and $F(\psi) = \{\partial H / \partial \mathbf{p}_i, -\partial H / \partial \mathbf{r}_i\} = \{\mathbf{p}_i / m_i, -\partial V / \partial \mathbf{r}_i\}$, so that Eq. (3) becomes

$$\frac{d\delta\psi}{dt} = \begin{pmatrix} \mathbf{0} & \mathbf{T} \\ -\mathbf{M} & \mathbf{0} \end{pmatrix} \delta\psi \quad (4)$$

with $\mathbf{T} = (T_{ij})$ the $3n \times 3n$ dimensional diagonal matrix whose elements are given by $T_{3i-2,3i-2} = T_{3i-1,3i-1} = T_{3i,3i} = 1/m_i$, \mathbf{M} the $3n \times 3n$ second derivative of the potential, namely the Hessian matrix $M_{ij} = \partial^2 V / \partial q_i \partial q_j$, and $\mathbf{0}$ the $3n \times 3n$ null matrix. Such an atomic system can be computationally studied with the standard tools of molecular dynamics (MD). Commonly used are the Verlet algorithm [39] to solve the equations of motion for the ‘‘physical’’ main trajectory, Eq. (1), and a fourth-order Runge-Kutta scheme to solve Eq. (3) for the ‘‘fiducial’’ tangent trajectory. Let us now come to the problem of molecular systems, more precisely made of linear molecules.

We consider a cluster made of n linear molecules. Each molecule i with mass m_i contains n_i atoms or entities, and we assume intramolecular bonds to be of fixed length. The molecular motion is split into the translation of the center of mass and the rotation about the center-of-mass contributions [40]. If molecule i has s_i interaction sites located on $\{\mathbf{r}_i^\alpha\}$, $1 \leq \alpha \leq s_i$, and if the force \mathbf{f}_i^α acts on site \mathbf{r}_i^α , the torque $\boldsymbol{\tau}_i$ about the center of mass \mathbf{r}_i is

$$\boldsymbol{\tau}_i = \sum_{\alpha=1}^{s_i} (\mathbf{r}_i^\alpha - \mathbf{r}_i) \times \mathbf{f}_i^\alpha \quad (5)$$

while the total force acting on \mathbf{r}_i is $\mathbf{f}_i = \sum_{\alpha} \mathbf{f}_i^\alpha$. In the following we denote by V the potential-energy function such that $\mathbf{f}_i^\alpha = -\partial V / \partial \mathbf{r}_i^\alpha$. We take advantage of the linearity of the molecules by using the fact that both angular velocity $\boldsymbol{\omega}_i$ and torque $\boldsymbol{\tau}_i$ must be perpendicular to the molecular axis \mathbf{e}_i . By writing $\mathbf{r}_i^\alpha - \mathbf{r}_i = d_i^\alpha \mathbf{e}_i$ for all i and α , we have [41]

$$\boldsymbol{\tau}_i = \mathbf{e}_i \times \mathbf{g}_i, \quad (6)$$

where we have defined \mathbf{g}_i as

$$\mathbf{g}_i = \sum_{\alpha=1}^{s_i} d_i^\alpha \mathbf{f}_i^\alpha. \quad (7)$$

Note that we can replace \mathbf{g}_i by its component perpendicular to \mathbf{e}_i without affecting Eq. (6), so that $\boldsymbol{\tau}_i = \mathbf{e}_i \times \mathbf{g}_i^\perp$ with

$$\mathbf{g}_i^\perp = \mathbf{g}_i - (\mathbf{g}_i \cdot \mathbf{e}_i) \mathbf{e}_i. \quad (8)$$

The first-order equations of translational motion are [40]

$$\frac{d\mathbf{r}_i}{dt} = \mathbf{v}_i, \quad (9)$$

$$\frac{d\mathbf{v}_i}{dt} = \mathbf{f}_i/m_i, \quad (10)$$

and the equations for rotational motion are [42]

$$\frac{d\mathbf{e}_i}{dt} = \mathbf{u}_i, \quad (11)$$

$$\frac{d\mathbf{u}_i}{dt} = \mathbf{g}_i^\perp/J_i + \gamma_i\mathbf{e}_i, \quad (12)$$

where J_i is the momentum of inertia and γ_i is a Lagrange multiplier to constrain bond lengths. The numerical propagation of vectors $\{\mathbf{e}_i\}$ and $\{\mathbf{u}_i\}$ from time $t - \delta t/2$ to δt lead, via a first-order Taylor expansion, to

$$\gamma_i(t)\delta t = -2\mathbf{u}_i(t - \delta t/2) \cdot \mathbf{e}_i(t), \quad (13)$$

which is equal, to the same order of approximation, to

$$\gamma_i(t)\delta t = -u_i^2(t)\delta t. \quad (14)$$

An efficient way to solve numerically Eqs. (9)–(12) has been proposed by Fincham [43]. It is based on a leap-frog algorithm which allows the direct estimation of γ_i at time t using Eq. (13).

To calculate the largest Lyapunov exponent λ of the cluster, we first define the current point ψ of the phase space, $\psi = \{\mathbf{r}_i, \mathbf{e}_i, \mathbf{v}_i, \mathbf{u}_i\}$. Similar to the atomic case, we write Eqs. (9)–(12) in condensed form $d\psi/dt = F(\psi)$. Suppose that a variation $\delta\psi(0)$ is imposed on ψ at time $t=0$. The time evolution of $\delta\psi$ is still governed by Eq. (3), but we have to illustrate the Jacobian $\partial F/\partial\psi$ according to Eqs. (9)–(12). We easily see that

$$\frac{\partial F}{\partial\psi} = \begin{pmatrix} \mathbf{0} & \mathbf{0} & \mathbf{1} & \mathbf{0} \\ \mathbf{0} & \mathbf{0} & \mathbf{0} & \mathbf{1} \\ \mathbf{A} & \mathbf{B} & \mathbf{0} & \mathbf{0} \\ \mathbf{C} & \mathbf{D} & \mathbf{0} & \mathbf{E} \end{pmatrix}, \quad (15)$$

where $\mathbf{A}, \mathbf{B}, \mathbf{C}, \mathbf{D}, \mathbf{E}$ are $3n \times 3n$ matrices to be determined and $\mathbf{1}$ is the $3n \times 3n$ identity matrix. The explicit derivation of these matrices is performed in the Appendix. As mentioned above, it is in principle possible to follow simultaneously the time evolution of $12n$ orthogonal vectors $\{\delta\psi_i\}$ in order to find all Lyapunov exponents. We expect that $14 + 2n$ of them would be zero due to conservation of the total energy, linear, and angular momenta (seven constants of the motion), but also due to the constraint of intermolecular bond lengths (n Lagrange multipliers).

III. APPLICATION TO SMALL NITROGEN CLUSTERS

In this section we illustrate the method formalized above to compute the largest Lyapunov exponent in clusters made of 3 and 13 nitrogen molecules. The potential chosen to model the interaction between N_2 molecules was previously used in bulk studies [44]. A Buckingham term acts between

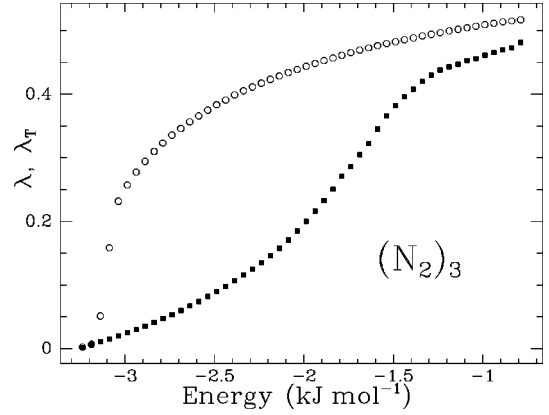


FIG. 1. Largest Lyapunov exponents in the $(\text{N}_2)_3$ cluster. The global Lyapunov exponent λ (open circles) and its translational restriction λ_T (full squares) are plotted against the total energy E in classical molecular-dynamics simulations. E is given in kJ mol^{-1} .

two nitrogen atoms of any different molecules, $V_B(r) = A \exp(-\alpha r) - C/r^6$, where the parameters A , α , C are taken as $A = 125\,502.7 \text{ kJ mol}^{-1}$, $\alpha = 3.461\,136 \text{ \AA}^{-1}$, and $C = 1641.2749 \text{ kJ \AA}^6 \text{ mol}^{-1}$. Multipolar interaction is modeled as four partial Coulombic charges located on the molecular axis. The two positive charges $0.373q_e$ are located at $\pm 0.847 \text{ \AA}$, the two negative charges $-0.373q_e$ at $\pm 1.044 \text{ \AA}$, with q_e the electronic charge. This description is complete with the intermolecular N-N bond length, 1.094 \AA . The same potential was used in previous thermodynamical investigations on $(\text{N}_2)_{13}$ and $(\text{N}_2)_{55}$ clusters [12,14]. A time step of 5 fs is used in classical isoergic MD simulations. At each total energy, the first 5 ns are retained for thermalization. The calculation of the largest Lyapunov exponent λ is then initiated, and from the subsequent 10 ns of the simulation, only the last 5 ns are kept for an average value of λ .

Besides λ calculated as a function of total energy for the $(\text{N}_2)_n$ cluster ($n=3$ or 13), we also evaluate a translational exponent λ_T by propagating a $6n$ -vector $\delta\psi_T(t)$ according to the following equation, similar to Eq. (4):

$$\frac{d\delta\psi_T}{dt} = \begin{pmatrix} \mathbf{0} & \mathbf{1} \\ \mathbf{A} & \mathbf{0} \end{pmatrix} \delta\psi_T, \quad (16)$$

where the $3n \times 3n$ matrix \mathbf{A} is given in Eq. (A1). Since λ_T refers only to a subset of coordinates in phase space, it is *not* a Lyapunov exponent in the usual sense, but simply a quantity that we hope to be sensitive only to the translational motion of the molecules.

All simulations are performed with zero total linear and angular momenta. To interpret our results physically, several geometrical parameters are calculated. First, we calculate the root mean square bond length fluctuation δ , also known as the Lindemann parameter. Moreover, an orientational order parameter α is defined as

$$\alpha = \langle \cos \theta \rangle = \lim_{T \rightarrow \infty} \frac{1}{T} \int_0^T \frac{1}{n} \sum_{i=0}^n \mathbf{e}_i(t) \cdot \mathbf{e}_i(0) dt. \quad (17)$$

We have plotted in Fig. 1 the largest Lyapunov exponent λ and its translational analog λ_T for the trimer $(\text{N}_2)_3$. At very

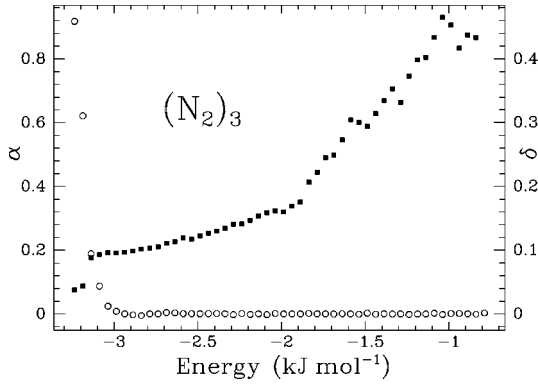


FIG. 2. Orientational order parameter α (open circles) and Lindemann parameter δ (full squares) versus total energy for $(\text{N}_2)_3$.

low energy, both exponents grow very softly from 0 and have very close values. When the energy reaches $E_0 \approx -3.1 \text{ kJ mol}^{-1}$, the curves become divergent and λ abruptly rises while λ_T still increases linearly. Finally, inflections occur for both λ and λ_T , but at a much lower energy for λ than for λ_T (near -1.5 kJ mol^{-1}). Furthermore, this inflection is much sharper for λ . In the whole range of energies we have $\lambda \geq \lambda_T$. From Fig. 2 we see that the lowest energy region is ordered, both orientationally and translationally. The orientational order is lost at $E \sim E_0$, and δ rises slightly. However, the translational order is lost at $E \approx -1.7 \text{ kJ mol}^{-1}$. Thus it appears that the Lyapunov exponent λ is mostly sensitive to the freedom of molecular rotation. Also essential is the contribution of the rotational terms (matrices **C**, **D**, and **E**) in the Jacobian $\partial F/\partial \psi$.

We observe in Fig. 3 similar qualitative behaviors of the Lyapunov exponents. From the variations of both α and δ presented in Fig. 4, we see that the system is fully rigid at low temperature, and that the centers of mass remain vibrating around the icosahedral geometry. In this region, the molecular axes also keep vibrating inside cones. Both Lyapunov exponents λ and λ_T have very low values. At $E = -41 \text{ kJ mol}^{-1}$, the loss of orientational order is accompanied by a strong rise in λ , but not in λ_T . When the cluster melts, near $E = -28 \text{ kJ mol}^{-1}$ (δ rises over 0.1), λ_T roughly reaches a maximal value. But, again, no signature of melting

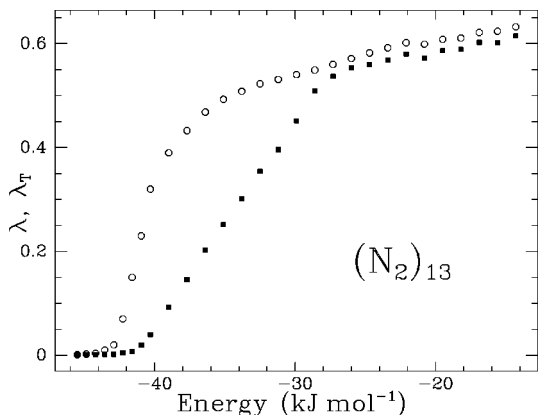


FIG. 3. Largest Lyapunov exponents in the $(\text{N}_2)_{13}$ cluster. The global Lyapunov exponent λ (open circles) and its translational restriction λ_T (full squares) are plotted against the total energy E in classical molecular-dynamics simulations. E is given in kJ mol^{-1} .

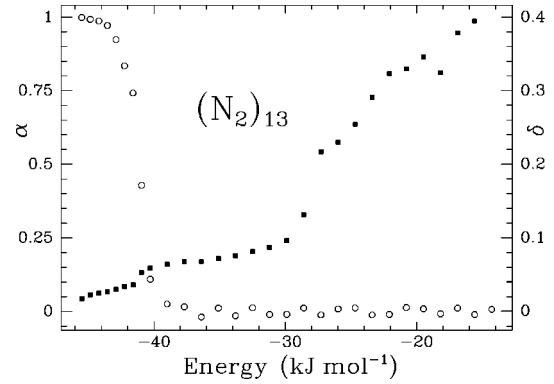


FIG. 4. Orientational order parameter α (open circles) and Lindemann parameter δ (full squares) versus total energy for $(\text{N}_2)_{13}$.

is seen on the variations of λ . On the contrary, λ seems to have reached the same upper limit, at a much lower energy, however. These variations are to be compared to those in other van der Waals clusters such as LJ clusters, where λ does not seem to show such an upper limit.

From these results, it appears that λ_T can be a fairly good approximation to the real exponent λ . This is especially true in the lowest- and highest-energy regimes. When the energy is low enough, the rotational degrees of freedom are nearly frozen, and contribute poorly to the divergence of $\delta\psi_T$: both exponents λ and λ_T are small. After the release of the internal degrees of freedom, λ soon reaches its upper limit while λ_T still increases regularly with energy. Once the solid-liquid transition has occurred, the rotational degrees of freedom evolve on a much faster time scale than the translational ones. As a consequence, fluctuations of the curvature on the potential-energy surface also become faster. In the limit of the high-energy regime, when the cluster is in its liquidlike state, the matrix **A** changes with the same rate as the other matrices of the Jacobian. This kind of ‘‘averaging effect’’ causes the parametric instabilities created by these fluctuations [28] to be of the same magnitude for both $\delta\psi$ and $\delta\psi_T$, hence producing similar values for λ and λ_T in this limit.

Therefore, the degree of chaos seen from the largest Lyapunov exponent in small nitrogen clusters is primarily driven by the orientational degrees of freedom. It should, however, be noted that, due to the separation between translational and rotational degrees of freedom in such clusters, the whole Lyapunov spectrum should carry much more useful information than the largest exponent alone. In particular, the Kolmogorov entropy might be a good parameter for investigating both phase transitions exhibited by these systems. Further insight would probably be gained by investigating other systems which do not exhibit an orientational transition, such as carbon dioxide clusters [12–14].

IV. CONCLUSION

We have illustrated a method for computing Lyapunov exponents in Hamiltonian systems made of linear molecules, from numerical experiments with classical molecular-dynamics simulations. In our study, we have only calculated the largest Lyapunov exponent λ . The other exponents and even the whole Lyapunov spectrum can be estimated in the same way with a regular orthonormalization procedure. The

present formulation explicitly uses the leapfrog algorithm of Fincham [43] to propagate the current trajectory in microcanonical MD. This approach is rather straightforward, and avoids the use of more intricate methods such as quaternions [45], which are somewhat redundant in the case of linear molecules. Recently, Dullweber *et al.* proposed a new method for dealing with molecular dynamics of systems made of rigid bodies [46]. This method seems more efficient and faster than the standard quaternions scheme, and will be developed to calculate Lyapunov exponents. This will be the subject of another communication.

We have computed λ versus total energy in small nitrogen clusters made of 3 and 13 molecules. These clusters are known to display a solid-solid phase transition, happening with the release of the molecular orientational degrees of freedom, embryonic of the bulk solid-plastic transition [12]. The orientational disorder occurs at a much lower energy than the energy required to isomerize or to melt. It has also been shown that this phenomenon may be characterized with thermal changes. Here we have observed that the Lyapunov exponent sharply rises when the orientational degrees of freedom are released, but also that it is not sensitive to melting. Moreover, λ seems to reach an upper limit at high energy. This is a very peculiar behavior for van der Waals clusters, but was seen to occur in ionic clusters [3]. Thus the specific dynamical behavior of molecular clusters may be suitably investigated using Lyapunov exponents as parameters and probes of some phase transitions, even if all thermal changes may not necessarily be associated to changes in λ .

The method developed in this work could be effectively used in the computation of Lyapunov exponents in other systems of linear molecules, and interacting through a classical many-body potential, possibly including more intricate effects such as Axilrod-Teller forces [27]. The application to clusters, of course, but also to periodic systems such as those investigated by Posch and Hoover [30] and by Kwon and Park [29] is rather straightforward. It would then allow investigations on more realistic models, in order to improve our understanding of how the chaotic properties change during a phase transition.

ACKNOWLEDGMENTS

The author wishes to thank Dr. J.-B. Maillet and Dr. A. Boutin for many helpful discussions. This work was supported by the CNRS, the Région Midi-Pyrénées, the Université Paul Sabatier, and the MENESR.

APPENDIX: CALCULATION OF THE JACOBIAN

In this appendix, we illustrate the five $3n \times 3n$ matrices **A**, **B**, **C**, **D**, and **E** of the $12n \times 12n$ Jacobian, Eq. (15). We assume the existence of a potential-energy function V such that the total force acting on the site α of molecule i (located at \mathbf{r}_i^α) can be written as $\mathbf{f}_i^\alpha = -\partial V / \partial \mathbf{r}_i^\alpha$. From Eq. (10) we find a straightforward expression for **A**, identical to the atomic case:

$$A_{ij} = -\frac{1}{m_i} \sum_{\alpha=1}^{s_i} \frac{\partial^2 V}{\partial q_i^\alpha \partial q_j}, \quad \forall i, j \quad (\text{A1})$$

with q_i any of the $3n$ coordinates of the center-of-mass positions $\{\mathbf{r}_i\} = \{x_i, y_i, z_i\}$. **B** can also be easily derived as

$$B_{ij} = -\frac{1}{m_i} \sum_{\alpha=1}^{s_i} \frac{\partial^2 V}{\partial q_i^\alpha \partial k_j}, \quad \forall i, j \quad (\text{A2})$$

with k_j any of the $3n$ coordinates of the axes orientations $\{\mathbf{e}_i\} = \{e_i^x, e_i^y, e_i^z\}$.

To find expressions for **C** and **D**, we must develop the variations of \mathbf{g}_i^\perp when ψ changes. Considering at the present time only the variations of \mathbf{g}_i [see Eq. (7)], we define the $3n \times 3n$ matrices **C**₀ and **D**₀ such that

$$C_0^{ij} = -\sum_{\alpha=1}^{s_i} d_i^\alpha \frac{\partial^2 V}{\partial q_i^\alpha \partial q_j}, \quad \forall i, j, \quad (\text{A3})$$

$$D_0^{ij} = -\sum_{\alpha=1}^{s_i} d_i^\alpha \frac{\partial^2 V}{\partial q_i^\alpha \partial k_j}, \quad \forall i, j. \quad (\text{A4})$$

To obtain the variations of \mathbf{g}_i^\perp from those of $\{\mathbf{r}_j\}$ and $\{\mathbf{e}_j\}$, we use the definition Eq. (8):

$$\delta \mathbf{g}_i^\perp = \delta \mathbf{g}_i - \mathbf{e}_i \delta(\mathbf{g}_i \cdot \mathbf{e}_i) - (\mathbf{g}_i \cdot \mathbf{e}_i) \delta \mathbf{e}_i. \quad (\text{A5})$$

It is useful to treat simultaneously the variations from $\{\mathbf{r}_j\}$ and $\{\mathbf{e}_j\}$, and to pose the $3n \times 6n$ matrix $\mathbf{M}_0 = (\mathbf{C}_0 | \mathbf{D}_0)$. We also define four $3n \times 3n$ block diagonal matrices (\mathbf{M}_j) , $1 \leq j \leq 4$, by

$$\mathbf{M}_j = \begin{pmatrix} \mathbf{L}_j^1 & & \mathbf{0} \\ & \ddots & \\ \mathbf{0} & & \mathbf{L}_j^n \end{pmatrix}, \quad (\text{A6})$$

where the $n \times n$ matrices (\mathbf{L}_j^i) , $1 \leq j \leq 4$, $1 \leq i \leq n$, are defined as

$$\mathbf{L}_1^i = \begin{pmatrix} e_i^x & & 0 \\ & e_i^y & \\ 0 & & e_i^z \end{pmatrix}, \quad (\text{A7})$$

$$\mathbf{L}_2^i = \begin{pmatrix} e_i^x & e_i^y & e_i^z \\ e_i^x & e_i^y & e_i^z \\ e_i^x & e_i^y & e_i^z \end{pmatrix}, \quad (\text{A8})$$

$$\mathbf{L}_3^i = (\mathbf{g}_i \cdot \mathbf{e}_i) \mathbf{1}, \quad (\text{A9})$$

$$\mathbf{L}_4^i = \begin{pmatrix} g_i^x e_i^x & & 0 \\ & g_i^y e_i^y & \\ 0 & & g_i^z e_i^z \end{pmatrix}. \quad (\text{A10})$$

We also introduce the $3n \times 6n$ matrix $\mathbf{M}_5 = (\mathbf{0} | \mathbf{M}_3 + \mathbf{M}_4)$. With all these definitions, one can show that the variations of $\{\mathbf{g}_i^\perp\}$ induced by those of $\{\mathbf{r}_j\}$ and $\{\mathbf{e}_j\}$ are bound through the linear relationship (at first order of perturbation):

$$\begin{pmatrix} \delta \mathbf{g}_i^\perp \\ \vdots \\ \delta \mathbf{g}_n^\perp \end{pmatrix} = (\mathbf{M}_0 - \mathbf{M}_1 \mathbf{M}_2 \mathbf{M}_0 - \mathbf{M}_5) \begin{pmatrix} \delta \mathbf{r}_1 \\ \vdots \\ \delta \mathbf{r}_n \\ \delta \mathbf{e}_1 \\ \vdots \\ \delta \mathbf{e}_n \end{pmatrix}. \quad (\text{A11})$$

It remains to study the contribution of the Lagrange multiplier term on the right-hand side of Eq. (12). Equation (13) is used in practice to compute γ_i at time t , from $\mathbf{u}_i(t - \delta t/2)$ and $\mathbf{e}_i(t)$. The knowledge of the multipliers $\{\gamma_i\}$ allows us to add the contribution $\gamma_i \delta \mathbf{e}_i$ to the variations of $d\delta \mathbf{u}_i/dt$, under the form of the $3n \times 6n$ matrix $\mathbf{M}_6 = (\mathbf{0} | \mathbf{\Gamma})$, with $\mathbf{\Gamma}$ the $3n \times 3n$ diagonal tensor:

$$\mathbf{\Gamma} = \begin{pmatrix} \mathbf{L}_5^1 & & \mathbf{0} \\ & \ddots & \\ \mathbf{0} & & \mathbf{L}_5^n \end{pmatrix}, \quad \text{where } \mathbf{L}_5^i = \gamma_i \mathbf{1}. \quad (\text{A12})$$

Finally we have obtained the explicit formulation of the matrices \mathbf{C} and \mathbf{D} :

$$(\mathbf{C} | \mathbf{D}) = \left(\frac{1}{J_i} \right) (\mathbf{M}_0 - \mathbf{M}_1 \mathbf{M}_2 \mathbf{M}_0 - \mathbf{M}_5) + \mathbf{M}_6, \quad (\text{A13})$$

where the factor $(1/J_i)$ must be applied to the rows $3i-2$, $3i-1$, and $3i$ for $1 \leq i \leq n$.

To find an expression for the block diagonal matrix \mathbf{E} , we can differentiate Eq. (14) to finally obtain

$$\mathbf{E} = -2 \begin{pmatrix} \mathbf{L}_6^1 & & \mathbf{0} \\ & \ddots & \\ \mathbf{0} & & \mathbf{L}_6^n \end{pmatrix},$$

where

$$\mathbf{L}_6^i = \begin{pmatrix} e_i^x u_i^x & e_i^x u_i^y & e_i^x u_i^z \\ e_i^y u_i^x & e_i^y u_i^y & e_i^y u_i^z \\ e_i^z u_i^x & e_i^z u_i^y & e_i^z u_i^z \end{pmatrix}. \quad (\text{A14})$$

All the matrices shown above can be calculated analytically for any effective two-body atom-atom intermolecular potential. Their expressions are valid at current time t . Since the leap-frog algorithm propagates the velocities from time $t - \delta t/2$ to time $t + \delta t/2$, the valuations of the matrix \mathbf{E} requires the extra valuation of the rotational velocities at time t .

-
- [1] A. Heidenreich, I. Schek, D. Scharf, and J. Jortner, *Z. Phys. D* **20**, 227 (1991); J. P. Rose and R. S. Berry, *J. Chem. Phys.* **96**, 517 (1992); **98**, 3246 (1993); **98**, 3262 (1993).
- [2] J. Luo, U. Landman, and J. Jortner, in *Physics and Chemistry of Small Clusters*, Vol. 158 of *NATO Advanced Study Institute Series B: Physics*, edited by P. Jena, B. K. Rao, and S. Khanna (Plenum, New York, 1987), p. 155.
- [3] F. Calvo and P. Labastie, *J. Phys. Chem. B* **102**, 2051 (1998).
- [4] R. Poteau, F. Spiegelmann, and P. Labastie, *Z. Phys. D* **30**, 157 (1994).
- [5] S. G. Kim and D. Tománek, *Phys. Rev. Lett.* **72**, 2418 (1994).
- [6] D. J. Wales, *J. Chem. Phys.* **101**, 3750 (1994).
- [7] D. J. Wales and I. Ohmine, *J. Chem. Phys.* **98**, 7257 (1993).
- [8] C. J. Tsai and K. D. Jordan, *J. Chem. Phys.* **99**, 6957 (1993).
- [9] A. Boutin, J.-B. Maillet, and A. H. Fuchs, *J. Chem. Phys.* **99**, 9944 (1993).
- [10] A. Boutin, B. Rousseau, and A. H. Fuchs, *Europhys. Lett.* **18**, 245 (1992).
- [11] A. Boutin, A. H. Fuchs, M.-F. de Feraudy, and G. Torchet, *J. Chem. Phys.* **105**, 3671 (1996).
- [12] J.-B. Maillet, A. Boutin, and A. H. Fuchs, *Phys. Rev. Lett.* **76**, 4336 (1996).
- [13] J.-B. Maillet, A. Boutin, and A. H. Fuchs, *Mol. Simul.* **19**, 285 (1997).
- [14] J.-B. Maillet, A. Boutin, S. Buttefey, F. Calvo, and A. H. Fuchs, *J. Chem. Phys.* **109**, 329 (1998).
- [15] T. L. Beck, D. M. Leitner, and R. S. Berry, *J. Chem. Phys.* **89**, 1681 (1988).
- [16] R. J. Hinde, R. S. Berry, and D. J. Wales, *J. Chem. Phys.* **96**, 1376 (1992).
- [17] C. Amitrano and R. S. Berry, *Phys. Rev. Lett.* **68**, 729 (1992).
- [18] D. J. Wales and R. S. Berry, *J. Phys. B* **24**, L351 (1991).
- [19] R. J. Hinde and R. S. Berry, *J. Chem. Phys.* **99**, 2942 (1993).
- [20] R. S. Berry, *J. Phys. Chem.* **98**, 6910 (1994).
- [21] S. K. Nayak, R. Ramaswamy, and C. Chakravarty, *Phys. Rev. E* **51**, 3375 (1995).
- [22] S. K. Nayak and R. Ramaswamy, *J. Phys. Chem.* **98**, 9260 (1994).
- [23] G. M. Tanner, A. Bhattacharya, S. K. Nayak, and S. D. Mahanti, *Phys. Rev. E* **55**, 322 (1997).
- [24] V. M. F. Morais and A. J. C. Varandas, *J. Phys. Chem.* **96**, 5704 (1992).
- [25] Y. Yurtsever, *Europhys. Lett.* **37**, 91 (1997).
- [26] F. Calvo, *J. Chem. Phys.* **108**, 6861 (1998).
- [27] C. Chakravarty, R. J. Hinde, D. M. Leitner, and D. J. Wales, *Phys. Rev. E* **56**, 363 (1997).
- [28] V. Mehra and R. Ramaswamy, *Phys. Rev. E* **56**, 2508 (1997).
- [29] K.-H. Kwon and B.-Y. Park, *J. Chem. Phys.* **107**, 5171 (1997).
- [30] H. A. Posch and W. G. Hoover, *Phys. Rev. A* **39**, 2175 (1989).
- [31] D. J. Wales, *Mol. Phys.* **78**, 151 (1993).
- [32] P. Butera and G. Caravati, *Phys. Rev. A* **36**, 962 (1987).
- [33] A. Bonasera, V. Latora, and A. Rapisarda, *Phys. Rev. Lett.* **75**, 3434 (1995).
- [34] L. Casetti, R. Livi, and M. Pettini, *Phys. Rev. Lett.* **74**, 375 (1995); L. Casetti, C. Clementi, and M. Pettini, *Phys. Rev. E* **54**, 5969 (1996).
- [35] I. Shimada and T. Nagashima, *Prog. Theor. Phys.* **61**, 1605 (1979).
- [36] G. Benettin, L. Galgani, and J.-M. Strelcyn, *Phys. Rev. A* **14**, 2338 (1974).

- [37] Y. Frøyland and K. H. Alfsen, *Phys. Rev. A* **29**, 2928 (1984).
- [38] H. D. Meyer, *J. Chem. Phys.* **84**, 3147 (1986).
- [39] L. Verlet, *Phys. Rev.* **159**, 98 (1967).
- [40] H. Goldstein, *Classical Mechanics* (Addison-Wesley, Reading, 1980).
- [41] M. P. Allen and D. J. Tildesley, *Computer Simulations of Liquids* (Oxford University Press, Oxford, 1987).
- [42] K. Singer, A. Taylor, and J. V. L. Singer, *Mol. Phys.* **33**, 1757 (1977).
- [43] D. Fincham, Daresbury Laboratory Quarterly for MD and MC Simulations, Report No. 12 (1984), p. 47.
- [44] H.-J. Böhm and R. Ahlrichs, *Mol. Phys.* **55**, 1159 (1985).
- [45] D. J. Evans, *Mol. Phys.* **34**, 317 (1977).
- [46] A. Dullweber, B. Leimkuhler, and R. McLachlan, *J. Chem. Phys.* **107**, 5840 (1997).